Science of the Total Environment xxx (2010) xxx–xxx

Contents lists available at ScienceDirect

Science of the Total Environment

journal homepage: www.elsevier.com/locate/scitotenv

Assessing the impact of waterborne and dietborne cadmium toxicity on susceptibility risk for rainbow trout

Chung-Min Liao [a,*], Yun-Ru Ju [a], Wei-Yu Chen [a], Bo-Ching Chen [b]

[a] Department of Bioenvironmental Systems Engineering, National Taiwan University, Taipei, 10617, Taiwan, ROC
[b] Department of Post-Modern Agriculture, Mingdao University, Changhua, 52345, Taiwan, ROC

ARTICLE INFO

Article history:
Received 30 June 2010
Received in revised form 24 October 2010
Accepted 26 October 2010
Available online xxxx

Keywords:
Cadmium
Ecotoxicology
Modeling
Susceptibility
Rainbow trout
Risk

ABSTRACT

The purpose of this study was to use a risk-based integrated-scale toxicological model to examine the impact of waterborne and dietborne cadmium (Cd) toxicity on rainbow trout (*Oncorhynchus mykiss*) susceptibility appraised with recent published data. A probabilistic assessment model was performed to estimate Cd susceptibility risk. The dose–response models were constructed based on two endpoints of % Cd in metabolically active pool (MAP) and susceptibility time that causes 50% effect (ST50). We further constructed an elimination–detoxification–recovery scheme to enhance the model predictive ability. We found a 95% probability of % Cd in gill and liver MAP exceeding 47–49% and it was likely (70% probability) to have exceeded 52–55%, but it was unlikely (30% probability) to have exceeded 56–60%. In contrast to gill and liver, gut had a relative lower Cd susceptibility risk (15–17% Cd in MAP) with a longer ST50. We suggested that the proposed probabilistic risk assessment framework can incorporate the elimination–detoxification–recovery scheme to help government based biomonitoring and bioassessment programs to prevent potential aquatic ecosystems and human health consequences.

1. Introduction

Cadmium (Cd) is a non-essential trace metal. Cd can accumulate to hazardous levels in living organisms posing environmental and human-health risks, which governments seek to reduce or eliminate. Cd is strongly associated with mining and manufacturing operations, products, and hazardous waste sites (Menzie et al., 2009). Cd has a tendency to accumulate by aquatic organisms via waterborne and/or dietborne exposure pathways (Alquezar et al., 2007, 2008).

It has been recognized that total metal exposure may be similar in exposure via ingestion or via gills (Clearwater et al., 2002; Gundogdu et al., 2009). Dietborne metals can reduce survival, growth and reproduction of aquatic invertebrates and fish (Meyer et al., 2005; Gundogdu et al., 2009). Dietborne metals can also significantly affect accumulation and trophic transfer of metal in freshwater food webs (Karimi et al., 2007).

Thus the interaction between dietborne metals and gastrointestinal tract of aquatic organisms plays an important role in aquatic ecosystems. Recent researches have raised significant concerns with respect to dietborne Cd due in part to sublethal levels of Cd that can affect ion regulation and cause physiological disturbances in fish (Ng and Wood, 2008; Tan et al., 2010).

The environmental chemistry of metals strongly influences their fate and effects on organisms and ecological receptors. Site-specific bioavailability is important for evaluating exposure to metals. The biotic ligand model (BLM), deriving from the gill surface interaction model and the free ion activity model, has been widely used in the last decade to predict metal bioavailability on aquatic organisms (Bielmyer et al., 2007; Brix et al., 2010). The BLM has been successfully applied to predict both acute and chronic toxicities of metals and their bioavailability on aquatic organisms (De Schamphelaere and Janssen, 2002; Schwartz and Vigneault, 2007).

A biologically-based damage assessment model (DAM) has been recently used to describe the mode of toxic action of contaminants with rapid reversible binding to the target site as well as to those that act with irreversible binding (Lee et al., 2002; Ashauer et al., 2007). The DAM implicates that death occurs when cumulative damage reaches a critical level. The DAM thus provides a more comprehensive framework to investigate the time-dependent toxicity of chemical incorporating both chemical and damage accumulations. This is particularly true for real field exposures (Ashauer et al., 2007).

The toxicokinetics and toxicodynamics of metals depend on metal, form of metal or metal compound, and the organism's ability to regulate and/or store metal (Curis et al., 2009). The physiologically-based pharmacokinetic (PBPK) models are potentially powerful tools in quantitative risk assessments for target tissue dose estimates. These models can be useful for ecological risk assessments because the PBPK modeling permits the calculation of target tissue doses through integration of information on the external dose, the physiological

* Corresponding author. Tel.: +886 2 2363 4512; fax: +886 2 2362 6433.
E-mail address: cmliao@ntu.edu.tw (C.-M. Liao).

0048-9697/$ – see front matter © 2010 Elsevier B.V. All rights reserved.
doi:10.1016/j.scitotenv.2010.10.044

structure of species, and the biochemical properties of metals. The PBPK modeling of metals in an organism can extrapolate from effective tissue concentrations to whole-organism doses (Kraemer et al., 2008). The simplest PBPK model of Cd in rainbow trout came from Thomann et al. (1997). The use of the PBPK models in risk assessment has grown substantially in the last decade and should only increase in the future (Hartung, 2009).

Recent studies of the subcellular partitioning model (SPM) in aquatic organisms have led to conclusions regarding the significance of the subcellular fates of metals to the potential biological consequences of accumulated metals (Wang and Rainbow, 2006; Wang and Wang, 2008; Gimbert et al., 2008; Dubois and Hare, 2009; Kamunde, 2009; Ponton and Hare, 2010). Subcellular partitioning of metals in the organisms may serve as another suitable toxicity predictor compared with accumulation-based determinants, considering the complex binding of metals in different subcellular pools with different metal-binding ligands (Wang and Rainbow, 2006). It has been recognized that Cd associated with heat labile (sensitive) protein and organelle reflects greater potential for Cd to interfere with vital physiological processes, whereas Cd associated with heat stable protein and metal-rich granules could be accounted for a detoxifying ability (Dubois and Hare, 2009; Kamunde, 2009). The toxicological significance, however, had not been found in Cd associated with cellular debris.

Understanding the processes of waterborne and dietborne metal exposures on aquatic organisms response will require viewing it on several levels, including bioavailability, bioaccumulation, bioregulation, and detoxification in individual species (Fairbrother et al., 2007; Menzie et al., 2009). Thus, to better understand the processes driving metal toxicity and assess their potential impact on ecophysiological response after Cd exposures, a DAM in the BLM scheme linked the internal metal partitioning and the PBPK modeling is capable for examining the bioaccumulation and coping mechanisms in species. The present approach is a step in this direction and can be enhanced by existing ecotoxicological modeling methods and relevant experimental data. Thus, linking the SPM and the PBPK modeling with the BLM and the DAM, formulated by understanding of inherent interactions among metal stressors, receptors, and metal regulations of organisms, can be used to quantify metal bioavailability and damage accumulation incorporating subcellular metal distribution and toxicokinetics under a broad range of metal stressor-driven environment.

The purpose of this study was to examine the impact of Cd toxicity on rainbow trout (*Oncorhynchus mykiss*) appraised with recent published experimental data by mechanistically linking the BLM, the DAM, the PBPK model, and the SPM. A probabilistic risk assessment approach was also presented to estimate Cd susceptibility risk for rainbow trout exposed to environmentally relevant Cd concentrations. Here the biological model chosen, rainbow trout, is a common used model fish in ecotoxicological studies (Renner, 2008). The present approach can provide a window for the ecotoxicological scheme and opens the way for understanding how rainbow trout show ecophysiological responses and their associated risk to Cd exposure.

2. Materials and methods

2.1. Study data

A valuable dataset provided by Ng and Wood (2008) and Kamunde (2009) give us the unique opportunity to examine the linkages and correlations between toxicokinetics and subcellular partitioning. Ng and Wood (2008) and Kamunde (2009) have conducted organ-level accumulation and subcellular fractionation experiments to better understand the importance of intracellular Cd partitioning for accurate tissue burden-based toxicity assessment based on both waterborne and dietborne Cd exposures. Thus, the published data of Ng and Wood (2008) and Kamunde (2009) were reanalyzed. The data covered a wide range of physiological characterization such as uptake, elimination, and detoxification, which allowed the present analysis.

Briefly, Ng and Wood (2008) investigated the toxicity of dietborne Cd from the oligochaete worm *Lumbriculus variegates* to juvenile rainbow trout (10–12 g wet wt). The worm were exposed to waterborne Cd (as $Cd(NO_3)_2 \cdot 4H_2O$) of 0, 5, 20, and 200 μg L^{-1} for 1 week and the fish were fed this food with accumulating Cd of 0.6, 2.2, and 30.3 μg g^{-1} wet wt for 1 month. The gill, liver, gut, and kidney were chosen as the target organs.

On the other hand, Kamunde (2009) carried out an exposure experiment by using juvenile rainbow trout (10–15 g wet wt) exposed to low-to-near-lethal concentrations of 5, 25, and 50 μg L^{-1} Cd (as $Cd(NO_3)_2 \cdot 4H_2O$) for 96 h without feeding at temperature 12.5 ± 0.5 °C, pH 7.5, and dissolved oxygen 9.22 ± 0.04 mg L^{-1}. The characteristics of water chemistry were measured to be: Na 47.1, Ca 58.8, Mg 27.6, K 2.26, Cl 137.3, and sulfate 17.2 mg L^{-1}. The gill and liver were chosen as the target organs with measurements of 0.48 ± 0.07 and 0.17 ± 0.05 g wet wt, respectively.

To determine subcellular Cd fractionation, Ng and Wood (2008) and Kamunde (2009) separated the homogenates of target organs from rainbow trout by differential centrifugation. The chemical and heat treatments were separated into five operationally defined subcellular fractions. These five fractions included (i) cell debris, (ii) cellular organelles (including nuclei, mitochondria, microsomes–lysosomes), (iii) cytosolic proteins denatured by heat treatment (i.e., heat-labile proteins (HLP)), (iv) heat stable proteins (HSP), and (v) metal-rich granules (expressed as NaOH-resistant).

Data from the subcellular Cd partitioning were summed into metal-sensitive and detoxified metal compartments or referred to as metabolically active pool (MAP) and metabolically detoxified pool (MDP). Thus, two summed pools have recently proposed to represent bioactive and detoxified fractions in subcellular Cd partitioning. MDP comprises HSP and NaOH-resistant fractions. MAP comprises Cd-associated HLP, nuclei, mitochondria, and microsomes–lysosomes, each containing sites potentially vulnerable to Cd binding.

Here the environmentally relevant Cd concentration from the Environmental Protection Administration Executive Yuan in Taiwan (www.epa.gov.tw) was used as the Cd stress to estimate the Cd susceptibility risk for rainbow trout in Taiwan.

2.2. Mechanistic models

2.2.1. DAM

The DAM is based on three assumptions: (i) the accumulation of Cd in fish is described by the first-order biokinetic model; (ii) the proportion of Cd tissue burden in fish for inducing damage accumulation and damage recovery is proportional to the cumulative damage; and (iii) when the accumulative damage reaches to a critical effect level the death occurs.

In this study, the DAM can be described by three dynamic variables: internal cumulative damage ($D(t)$), cumulative hazard ($H(t)$), and susceptibility probability ($S(t)$). Firstly, $D(t)$ can be solved by incorporating the one-compartment toxicokinetic model $dC_b(t)/dt = k_1C_e - k_2C_b(t)$ into the damage accumulation model $dD(t)/dt = k_aC_b(t) - k_rD(t)$ as (Lee et al., 2002),

$$D(t) = k_a \frac{k_1}{k_2} C_e \left(\frac{e^{-k_r t} - e^{-k_2 t}}{k_r - k_2} + \frac{1 - e^{-k_r t}}{k_r} \right), \quad (1)$$

where $C_b(t)$ is the Cd burden in tissue in time t (μg g^{-1} wet wt), k_a is the damage accumulation rate (g μg^{-1} d^{-1}), k_r is the damage recovery rate constant (d^{-1}), k_1 is the rainbow trout uptake rate constant (mL g^{-1} d^{-1}), k_2 is the elimination rate constant of Cd (d^{-1}), and C_e is the exposure Cd

Please cite this article as: Liao C-M, et al, Assessing the impact of waterborne and dietborne cadmium toxicity on susceptibility risk for rainbow trout, Sci Total Environ (2010), doi:10.1016/j.scitotenv.2010.10.044

concentration in water ($\mu g\,L^{-1}$) or in diet ($\mu g\,g^{-1}$ wet wt). Here the recovery rate constant characterizes all processes leading to recovery such as repair mechanisms on a cellular scale or adaptation of the physiology and other compensating processes (Ashauer et al., 2007).

Secondly, an important DAM parameter referring to as the killing rate constant k_k ($g\,\mu g^{-1}\,d^{-1}$) is introduced. The killing rate constant is the proportionality factor describing the relation between the cumulative damage and cumulative hazard as

$$H(t) = (k_k / k_a)D(t). \tag{2}$$

Lastly, the susceptibility risk probability $S(t)$ can be derived directly from an exponential relationship of cumulative hazard as (Lee et al., 2002; Ashauer et al., 2007),

$$S(t) = 1 - exp(-H(t)) = 1 - exp\left[-k_k \frac{k_1}{k_2} C_e \left(\frac{e^{-k_r t} - e^{-k_2 t}}{k_r - k_2} + \frac{1 - e^{-k_r t}}{k_r}\right)\right]. \tag{3}$$

2.2.2. BLM-based DAM for gill

Here the BLM-based DAM was used to predict the degree of Cd binding at the site of action causing toxicity in gill of rainbow trout. There are three assumptions in the BLM: (i) the completion of the free metal ion with other naturally occurring cations (e.g., Ca^{2+}, Na^{+}, Mg^{2+}, and H^{+}) together with complexation by abiotic ligands (e.g., dissolved organic matter, carbonates) for binding with the biotic ligand; (ii) the site of toxic action on the organisms and the magnitude of the toxic effect are independent on the physiochemical characteristics of the medium, and (iii) the gills of organisms bear negatively charged ligands to which cationic metals can bind and constitute the primary sites for toxicity of most metals (De Schamphelaere and Janssen, 2002).

In the BLM scheme, the effect concentration for 50% response over time ($EC50_{BLM}(t)$) can be expressed in terms of time course fraction of the total number of Cd binding sites occupied by Cd at 50% effect ($f_{CdBL}^{50\%}(t)$) (De Schamphelaere and Janssen, 2002),

$$EC50_{BLM}(t) = \frac{f_{CdBL}^{50\%}(t)(1 + [a])}{(1 - f_{CdBL}^{50\%}(t))K_{CdBL}}, \tag{4}$$

where $[a] = K_{CaBL}\{Ca^{2+}\} + K_{MgBL}\{Mg^{2+}\} + K_{NaBL}\{Na^{+}\} + K_{HBL}\{H^{+}\}$ in that K_{CaBL}, K_{MgBL}, K_{NaBL}, and K_{HBL} represent the affinity constants for the binding of these cations to the biotic ligand (M^{-1}), {*ions*} denotes the activity of each ion of water chemistry characteristics (M), and K_{CdBL} represents the affinity constant of Cd binding to biotic ligand (M^{-1}).

The BLM and the DAM can be linked to construct a relation for estimating time-dependent $f_{CdBL}^{50\%}(t)$ by assuming that free ion activity concentration-caused 50% effect calculated by the DAM ($EC50_{DAM}(t)$) equals to that predicted by the BLM ($EC50_{BLM}(t)$) (Tsai et al., 2009),

$$\frac{D_{E,50}/k_a}{\left(\frac{e^{-k_r t} - e^{-k_2 t}}{k_r - k_2} + \frac{1 - e^{-k_r t}}{k_r}\right)} BCF^{-1} = \frac{f_{CdBL}^{50\%}(t)(1 + [a])}{(1 - f_{CdBL}^{50\%}(t))K_{CdBL}}, \tag{5}$$

where $D_{E,50}$ is the cumulative damage for 50% effect (−), and $D_{E,50}/k_a$ is a coefficient reflecting the compound equivalent toxic damage level required for 50% effect ($\mu g\,d\,g^{-1}$). The killing rate constant can be calculated as $k_k = \ln 2/(D_{E,50}/k_a)$ (Lee et al., 2002).

2.2.3. PBPK model

The present PBPK model used to estimate Cd concentrations in target organs can be modified from a prototypical Cd-rainbow trout PK model developed by Thomann et al. (1997). The PBPK model structure consisted of storage, gill, gut wall, kidney, liver, and alimentary cannel, which are interconnected by blood circulation (see Appendix A1). The essence of almost all the PBPK models can be described by a linear dynamic equation as

$$\frac{d\{C(t)\}}{dt} = [A]\{C(t)\} + [B]\{u(t)\}, \tag{6}$$

where $\{C(t)\}$ is the state variable vector describing Cd in each target organ ($\mu g\,g^{-1}$), $\{u(t)\}$ is the input vector of Cd in water ($\mu g\,L^{-1}$) and food ($\mu g\,g^{-1}$), $[A]$ is the state matrix describing the exchange rate between target organs ($L\,d^{-1}$), and $[B]$ is the constant input matrix describing the exchange rate into target organs ($L\,d^{-1}$). The detailed PBPK model equations are listed in Appendix A2.

2.3. Probabilistic susceptibility risk model

The time-dependent susceptibility risk probability $S(t)$ in Eq. (3) can be predicted under different exposed Cd concentrations and susceptibility time that causes 50% effect (ST50) for each exposed concentrations. Therefore, the relationship of tissue Cd burdens (C_b) and ST50 can be used to construct the dose–response profile for the risk assessment. Thus, this study used the relationships between C_b and % Cd fraction in MAP (% MAP) and ST50 to construct the organ-specific dose–response assessment models.

The dose–response profiles can be expressed mathematically as the conditional probabilities of $P(\%\ MAP|C_b)$ and $P(ST50|C_b)$, respectively. Given the fitted organ-specific dose–response models, susceptibility risk for specific organ can be calculated as the probability density functions (pdfs) of tissue Cd burden predicted from the PBPK model ($P(C_b)$) multiplied by the conditional probability of $P(\%\ MAP|C_b)$ or $P(ST50|C_b)$. Therefore, a joint probability function (JPF) can be used to calculate susceptibility risk probability,

$$P(R_{\%MAP}) = P(C_b) \times P(\%MAP|C_b), \tag{7a}$$

$$P(R_{ST50}) = P(C_b) \times P(ST50|C_b), \tag{7b}$$

where $P(R_{\%MAP})$ and $P(R_{ST50})$ represent the Cd susceptibility risk estimates based on two endpoints of % Cd in MAP and ST50, respectively.

2.4. Data analysis and model parameterization

Toxicokinetic parameters of uptake and elimination rate constants (k_1 and k_2) can be determined by fitting the integrated form of toxicokinetic rate equation to exposure data under constant waterborne and dietborne Cd,

$$C_b(t) = C_{b0}e^{-k_2 t} + \frac{k_1}{k_2} C_e \left(1 - e^{-k_2 t}\right), \tag{8}$$

where C_{b0} is initial concentration of Cd in target tissue of rainbow trout ($\mu g\,g^{-1}$ wet wt). In this study, the toxicokinetic model was used to fit the waterborne bioaccumulation data of gill and liver (Kamunde, 2009) and dietborne bioaccumulation data of gut (Ng and Wood, 2008), respectively. During the fitting procedure we incorporated different exposed concentrations (C_e) and time-varied tissue concentrations (C_b) into the model to estimate each concentration-, tissue-, and subcellular fraction-specific toxicokinetic parameters.

Detoxification rate (k_d, d^{-1}) can be estimated followed a metal influx threshold (MIT) concept introduced by Croteau and Luoma (2009). Croteau and Luoma (2009) proposed that MIT occurs when metal influx ≥ the combined rates of metal loss and detoxification. Based on the MIT perspective, k_d can be calculated as

$$k_d = \frac{k_1 C_e}{C_b} - k_{2,MAP}, \tag{9}$$

where $k_{2,MAP}$ is the Cd elimination rate constant in MAP (d^{-1}).

Please cite this article as: Liao C-M, et al, Assessing the impact of waterborne and dietborne cadmium toxicity on susceptibility risk for rainbow trout, Sci Total Environ (2010), doi:10.1016/j.scitotenv.2010.10.044

Here a Hill-based standard 4-parameter sigmoidal dose–response equation was used to fit the published data of % Cd in MAP–Cd exposure concentration in gill, liver, and gut to estimate EC50 and ED50 values in different exposed period, respectively,

$$R(C_e) = R_{min} + \frac{(R_{max} - R_{min})}{1 + \left(\frac{C_e}{E50}\right)^n}, \quad (10)$$

where $R(C_e)$ is the C_e-dependent response measured as % Cd in MAP (%), R_{min} and R_{max} are the minimum and maximum response (%), E50 is the effective concentration at 50% response, and n is the Hill coefficient.

The PBPK model is composed of terms involving physiological and physicochemical parameters. Physiological parameters needed for the rainbow trout PBPK model include tissue weights, growth rate, blood volume and the exchange rates between tissue compartments. It is not possible to estimate all of the parameters for the PBPK model independently of the experimental data. It is possible, however, to estimate from the literature, the order of parameters for the exchange rate between compartments and the physicochemical parameters, including organ-specific partition coefficients, gill sorption factors and the fraction of Cd in the available plasma form. Therefore, a preliminary database from Thomann et al. (1997) regarding Cd bioaccumulation in rainbow trout was adopted to estimate a range of model parameters with bioaccumulation data in lab reported in Ng and Wood (2008) and Kamunde (2009). Thomann et al. (1997) pointed out that the final set of parameters used to calibrate the data is hardly unique and variations may give equally reasonable calibration results.

Validity of the PBPK model of Cd was supported by reasonable agreement between model predictions and data for the concentration–time profiles of Cd in a variety of tissues. To compare modeled and observed results, the best fit was evaluated using root-mean-squared-error (RMSE), computed from RMSE $= \sqrt{\sum_{n=1}^{N}(C_{m,n} - C_{s,n})^2 / N}$ where N denotes the number of measurements, $C_{m,n}$ is the measurement data, and $C_{s,n}$ is the simulation result corresponding to data point n.

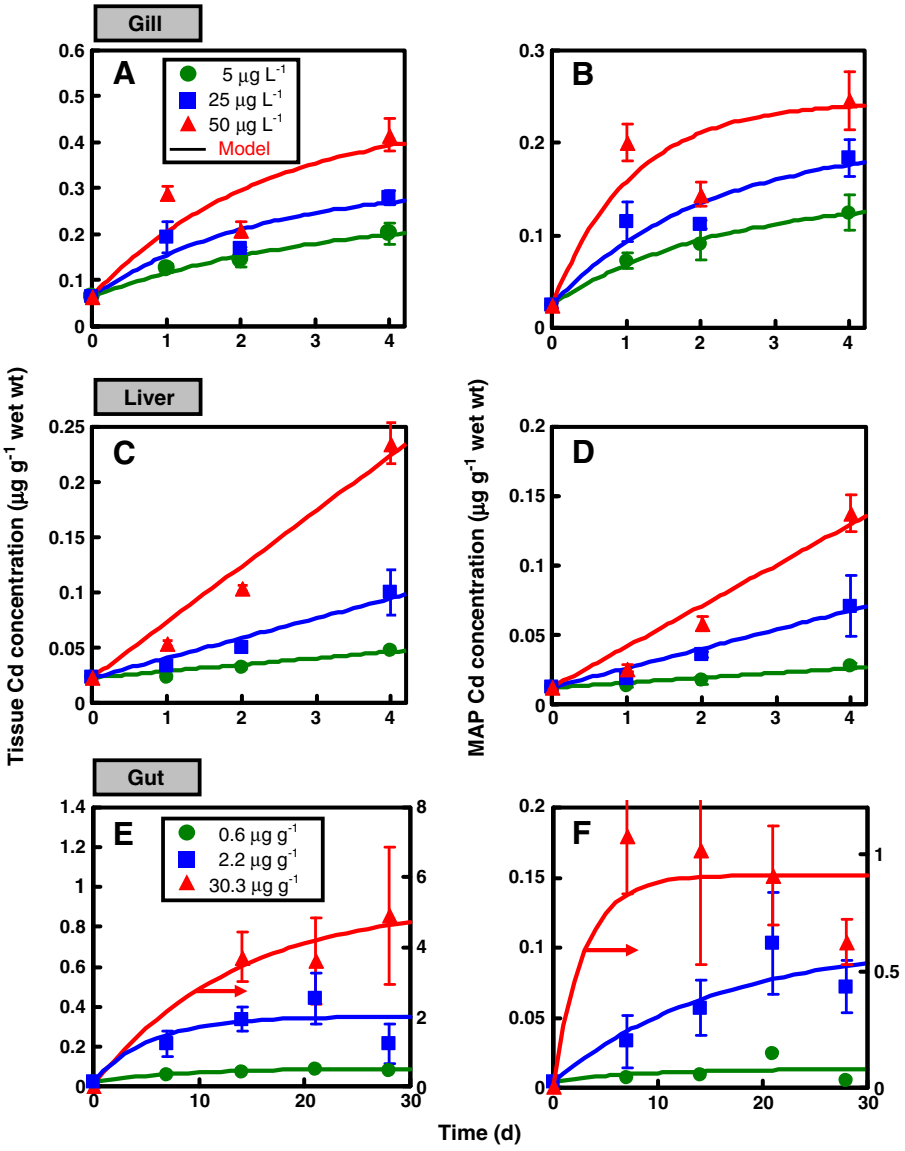

Fig. 1. Fitting toxicokinetic model (curves) to published exposure data of tissue (symbols of circle, square, and triangle) and metabolically active pool (MAP) in (A, B) gill and (C, D) liver exposed to 5, 25, and 50 μg L^{-1} waterborne Cd and in (E, F) gut exposed to 0.6, 2.2, and 30.3 μg g^{-1} dietborne Cd under exposure period. Solid curves indicate fitted model and error bars denote the standard deviation from mean. The data of gill and liver adpted from Kamunde (2009), whereas the data of gut adpted from Ng and Wood (2008). The data and model of concentration of 30.3 μg g^{-1} refer to the right vertical axis in (E) and (F).

Please cite this article as: Liao C-M, et al, Assessing the impact of waterborne and dietborne cadmium toxicity on susceptibility risk for rainbow trout, Sci Total Environ (2010), doi:10.1016/j.scitotenv.2010.10.044

Table 1
Fitted toxicokinetic, metal influx threshold model, damage assessment model parameters for target organs of gill, liver and gut exposed to waterborne and dietborne Cd.

	Gill			Liver			Gut		
	Cd in water ($\mu g\ L^{-1}$)						Cd in worm ($\mu g\ g^{-1}$ wet wt)		
	5	25	50	5	25	50	0.6	2.2	30.3
Toxicokinetic model									
k_1 ($mL\ g^{-1}\ d^{-1}$)	11.85	4.47	3.46	1.18	0.72	1.01	0.018	0.028	0.013
($g\ g^{-1}\ d^{-1}$)[a]	(2.26)[b]	(2.31)	(2.41)	(0.69)	(0.30)	(0.34)	(0.005)	(0.026)	(0.00073)
k_2 (d^{-1})	0.32	0.46	0.44	1.01×10^{-5}	6.08×10^{-6}	1.19×10^{-6}	0.124	0.185	0.0747
	(0.14)	(0.44)	(0.57)	(0.32)	(0.23)	(0.18)	(0.044)	(0.204)	(0.00686)
r^2	0.98	0.86	0.77	0.92	0.95	0.97	0.96	0.71	0.96
Metal influx threshold hypothesis									
$k_{1,MAP}$ ($mL\ g^{-1}\ d^{-1}$)	12.97	3.90	4.56	0.69	0.56	0.59	0.0024	0.0030	0.0103
($g\ g^{-1}\ d^{-1}$)[a]	(1.85)	(1.67)	(0.58)	(1.1)	(0.17)	(0.30)	(0.0008)	(0.0003)	(0.0011)
$k_{2,MAP}$ (d^{-1})	0.46	0.48	0.93	4.52×10^{-6}	1.26×10^{-7}	2.92×10^{-6}	0.1073	0.0625	0.3426
	(0.10)	(0.34)	(0.17)	(0.30)	(0.10)	(0.23)	(0.0447)	(0.0131)	(0.0405)
r^2	0.99	0.92	0.79	0.93	0.96	0.95	0.21	0.82	0.71
k_d (d^{-1})	0.45	1.23	1.72	0.26	0.8	2.24	2.24	13.57	87.42
Damage assessment model									
k_r (d^{-1})	1.45	1.08	1.12				1.85×10^{-6}	1.02×10^{-6}	1.37×10^{-2}
	(1.02)	(0.81)	(0.83)				(4.8×10^{-8})	(4.8×10^{-8})	(0.059)
k_k ($g\ \mu g^{-1}\ d^{-1}$)	0.09 (0.02)	0.23 (0.05)	0.30 (0.07)				0.095 (0.012)	0.069 (0.010)	0.118 (0.017)
r^2	0.98	0.98	0.98				0.99	0.99	0.99

[a] Unit for dietborne Cd exposure.
[b] Value in the parentheses denotes standard error from mean.

TableCurve 2D (Version 5.0) and 3D (Version 4.0) (AISN Software Inc., Mapleton, OR, USA) were used to perform the model fittings. A value of $p<0.05$ was judged significant. The WHAM (Windermere humic aqueous model) Version 6 (WHAM VI, Center for Ecology and Hydrology, Lancaster, UK) was performed to calculate the activities of competing and complex ions considered in the BLM scheme. A Monte Carlo technique was performed to generate 2.5th- and 97.5th-percentiles as the 95% confidence interval (CI) for all fitted models.

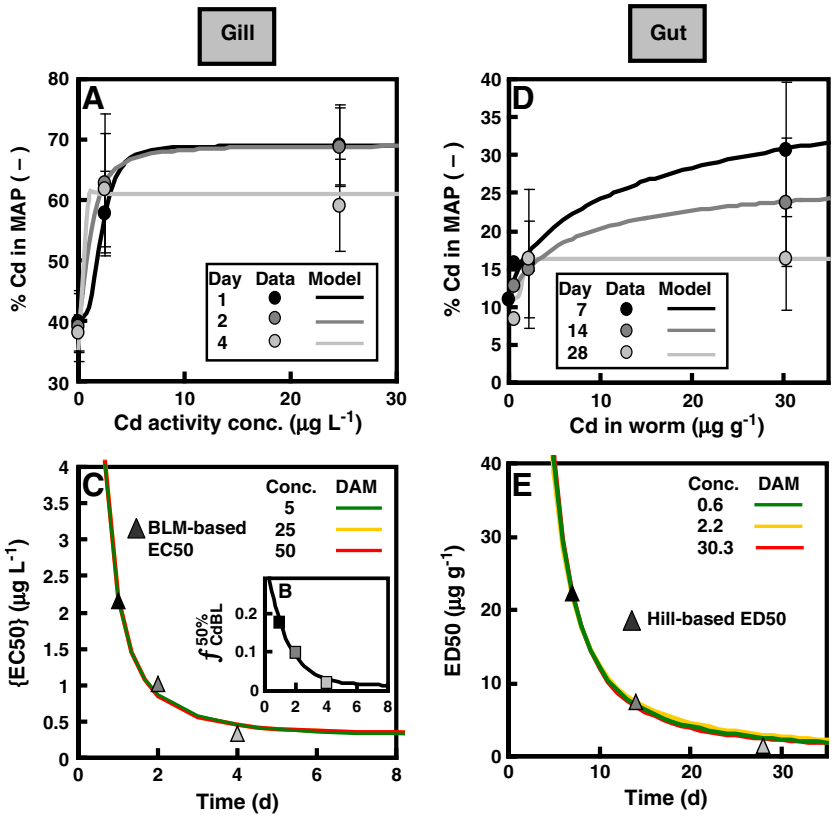

Fig. 2. (A) The relationship between % Cd in gill-MAP and Cd activity concentration under 1 (black), 2 (gray), and 4 (light gray) days exposure time fitted by a Hill model. (data adpted from Kamunde (2009)) (B) Predicted gill-$f^{50\%}_{CdBL}(t)$ varied with time by a best-fitting model to estimated BLM-based EC50. (C) Using DAM to fit BLM-based EC50 to estimate concentration-specific DAM parameters in 5, 25, and 50 $\mu g\ L^{-1}$ for gill. As well as for gut, (D) Hill model was used to fit the relationship between % Cd in MAP to dietborne Cd concentration under 7 (black), 21 (gray), and 28 (light gray) days exposure time (data adpted from Ng and Wood (2008)), and (E) fitting DAM to Hill-based ED50 data for dietborne 0.6, 2.2, and 30.3 $\mu g\ g^{-1}$ Cd.

Please cite this article as: Liao C-M, et al, Assessing the impact of waterborne and dietborne cadmium toxicity on susceptibility risk for rainbow trout, Sci Total Environ (2010), doi:10.1016/j.scitotenv.2010.10.044

Table 2
Fitted Hill model coefficients for % Cd in gill-MAP and Cd activity as well as gut-MAP and dietborne Cd relationships.

Hill model parameter	Gill			Gut		
	1 d	2 d	4 d	7 d	14 d	28 d
R_{min} (%)	39.76	39.11	35.62	10.99	10.99	11.13
R_{max}–R_{min} (%)	29.21	29.93	25.34	35.94	16.81	5.23
N	3.16	1.64	16.98	0.68	0.88	7.70
EC50 (μg L^{-1})	4.31	2.22	0.42			
ED50 (μg g^{-1} wet wt)				22.27	7.81	1.44
r^2	0.99	0.99	0.97	0.98	0.99	0.63

Largely because of limitations in the data used to derive model parameters, inputs were assumed to be independent. The result showed that 5000 iterations are sufficient to ensure the stability of results. The Crystal Ball® software (Version 2000.2, Decisionerring, Inc., Denver, Colorado, USA) was used to implement the Monte Carlo simulation.

3. Results

3.1. Parameter estimations

The sigmoidal uptake fashions were found in gill and gill-MAP when rainbow trout were exposed to waterborne Cd ranging from 5 to 50 μg L^{-1} over the course of exposure experiment (Fig. 1A, B). The linear uptake patterns, however, were found in liver and liver-MAP (Fig. 1C, D). On the other hand, the sigmoid fashions were found in gut and gut-MAP when rainbow trout exposed to dietborne Cd ranging from 0.6 to 30.3 μg g^{-1} wet wt (Fig. 1E, F).

The toxicokinetic equation in Eq. (8) was fitted to exposure data to obtain concentration-specific estimates of uptake and elimination rate constants k_1 and k_2, respectively, in gill, liver, gut, and MAP (Table 1; Fig. 1). Overall, k_1 estimates of gill and gill-MAP decreased with increasing of Cd concentrations ranging from 3.46 to 11.85 and 4.56 to 12.97 mL g^{-1} d^{-1}, respectively. However, k_2 of gill and gill-MAP increased with increasing of Cd concentrations ranging from 0.32 to 0.46 and 0.46 to 0.93 d^{-1}, respectively (Table 1). For liver and liver-MAP, k_1 estimates did not vary significantly with Cd concentrations (nearly 1 mL g^{-1} d^{-1} for liver and 0.6 mL g^{-1} d^{-1} for liver-MAP). Very low elimination rates with order of magnitudes 10^{-6}–10^{-5} were found, indicating that Cd in liver and liver-MAP can only be eliminated very slowly (Table 1). For gut, k_1 and k_2 estimates increased with increasing of Cd at low dietborne exposure, ranging from 0.018 to 0.028 d^{-1} and 0.124 to 0.185 d^{-1}, respectively, whereas at relative high dietborne exposure, low k_1 and k_2 estimates were found to be 0.013 and 0.0747 d^{-1}, respectively (Table 1). For gut-MAP, however, k_1 and k_2 estimates did not vary significantly with dietborne Cd exposures (Table 1).

Generally, estimated detoxification rate constants (k_d) were increased with increasing of Cd exposures. The resulting k_d estimates ranged from 0.45 to 1.72 and 0.26 to 2.24 d^{-1} for gill-MAP and liver-MAP, respectively, exposed to waterborne Cd of 5 to 50 μg L^{-1} over the course of exposure experiment (Table 1). For gut-MAP, k_d estimates ranged from 2.24 to 87.42 d^{-1} exposed to dietborne Cd of 0.6–30.3 μg g^{-1} wet wt (Table 1).

The Hill model (Eq. (10)) well described the relationships between % Cd in gill-MAP and Cd activity as well as gut-MAP and dietborne Cd (Fig. 2A, D; Table 2). Eq. (4) together with EC50(t) estimates in gill (Table 2) can be used to calculate $f_{CdBL}^{50\%}(t)$values based on known affinity constants and BLM parameters [a] and K_{CdBL} (see Appendix C). $f_{CdBL}^{50\%}(t)$ values were estimated to be 0.174, 0.098, and 0.02, respectively, for exposure time 1, 2, and 4 d. Fig. 2B shows $f_{CdBL}^{50\%}(t)$ over time with a best-fitting model $f_{CdBL}^{50\%}(t) = 0.14 + 0.34\exp(-t/1.33)$ ($r^2 = 0.99$, $p < 0.05$). Thus the best-fitted model of $f_{CdBL}^{50\%}(t)$ can be used to estimate BLM-based EC50 by Eq. (1), resulting in 2.16, 1.01, and 0.33 μg L^{-1} at days 1, 2, and 4, respectively (Fig. 2C).

Here Eq. (5) was used to fit estimated BLM-based EC50 and fitted Hill-based ED50 data to estimate Cd-specific DAM parameters of k_r and k_k for

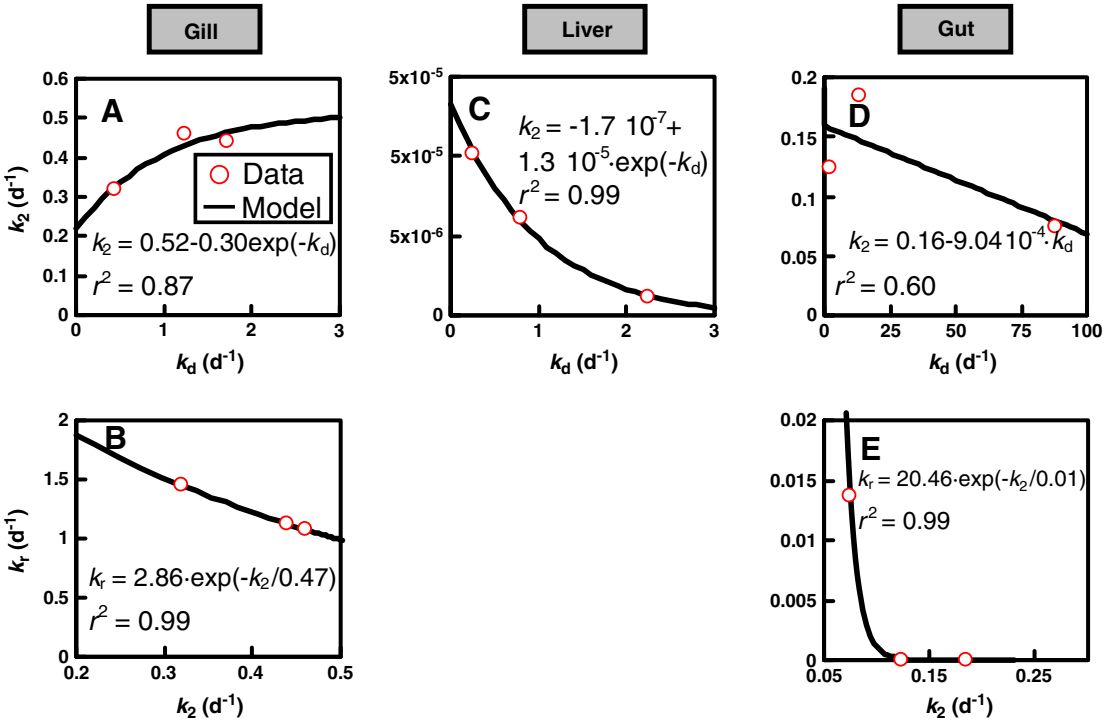

Fig. 3. Overall display of relationships among elimination rate (k_2), recovery rate (k_r), and detoxification rate (k_d) constants in target tissues. The relations of k_2–k_d and k_r–k_2 in (A, B) gill, (C) liver, and (D, E) gut.

Please cite this article as: Liao C-M, et al, Assessing the impact of waterborne and dietborne cadmium toxicity on susceptibility risk for rainbow trout, Sci Total Environ (2010), doi:10.1016/j.scitotenv.2010.10.044

gill and gut, respectively (Fig. 2C, E; Table 1). The results revealed that k_r estimates for gill ranged from 1.08 to 1.45 d^{-1}, whereas k_k estimates ranging from 0.09 to 0.30 $g\mu g^{-1}$ d^{-1} increased with increasing of Cd. On the other hand, low recovery rates were found in gut (10^{-6}–10^{-2} d^{-1}) with k_k estimates ranging from 0.095 to 0.118 $g\mu g^{-1}$ d^{-1} (Table 1).

3.2. Relationships among k_2, k_r, and k_d

An exponentially positive relationship between k_2 and k_d in gill were found (Fig. 3A). However, an exponentially negative relationship was found between k_r and k_2 in gill (Fig. 3B). For liver, however, only the k_2-k_d relations can be found with an exponentially negative trend, indicating that increasing k_d may compensate for lower k_2 (Fig. 3C). Fig. 3C also indicates that liver did not have an effective ability to eliminate Cd at a relative higher waterborne Cd, yet they performed a good ability to detoxify Cd. In contrast to gill, a negative linear relationship was found between the ability to eliminate dietborne Cd and the detoxifying ability in gut (Fig. 3D). Similarly, the gut k_r-k_2 relations also reveal an exponentially negative trend (Fig. 3E). Overall, Fig. 3 reveals that once k_2 is determined experimentally, k_r and k_d can be predicted by proposed fitted models.

3.3. Dose–response assessment

A best-fitting model in the form of $y=a(1-\exp(-bx))$ can describe the dose–response relationships between % Cd in MAP and Cd in tissues for gill, liver, and gut ($r^2=0.57-0.73$) (Fig. 4). To estimate dose-specific ST50 for gill and gut, the DAM in Eq. (3) can be used to calculate time-dependent susceptibility risk probability $S(t)$ (Fig. 5A, C). Given estimated dose-specific ST50 values for gill and gut, a best-fitted power function $y=ax^b$ well described the dose–response relationships between ST50 and Cd in tissue ($r^2=0.96-0.99$) (Fig. 5B, D).

3.4. Cd susceptibility risk estimates

To investigate the organ-specific Cd susceptibility risk probability for rainbow trout, the constructed organic-specific dose–response models for two endpoints of % Cd in MAP ($P(\%\ \mathrm{MAP}|C_b)$, Fig. 4) and ST50 ($P(\mathrm{ST50}|C_b)$, Fig. 5), respectively, were used. The environmentally relevant Cd concentration in Taiwan had a lognormal (LN) distribution with a geometric mean (gm) of 1.15 $\mu g\ L^{-1}$ and a geometric standard deviation (gsd) of 1.26 (Fig. 6A). We used data of Cd concentration in worm against Cd in water that adopted from Ng and Wood (2008) to fit linear relationship. Based on the linear relationship ($C_f=0.1511\ C_w$, $r^2=0.99$) (Fig. 6B), the probability distribution of Cd in worm subject to

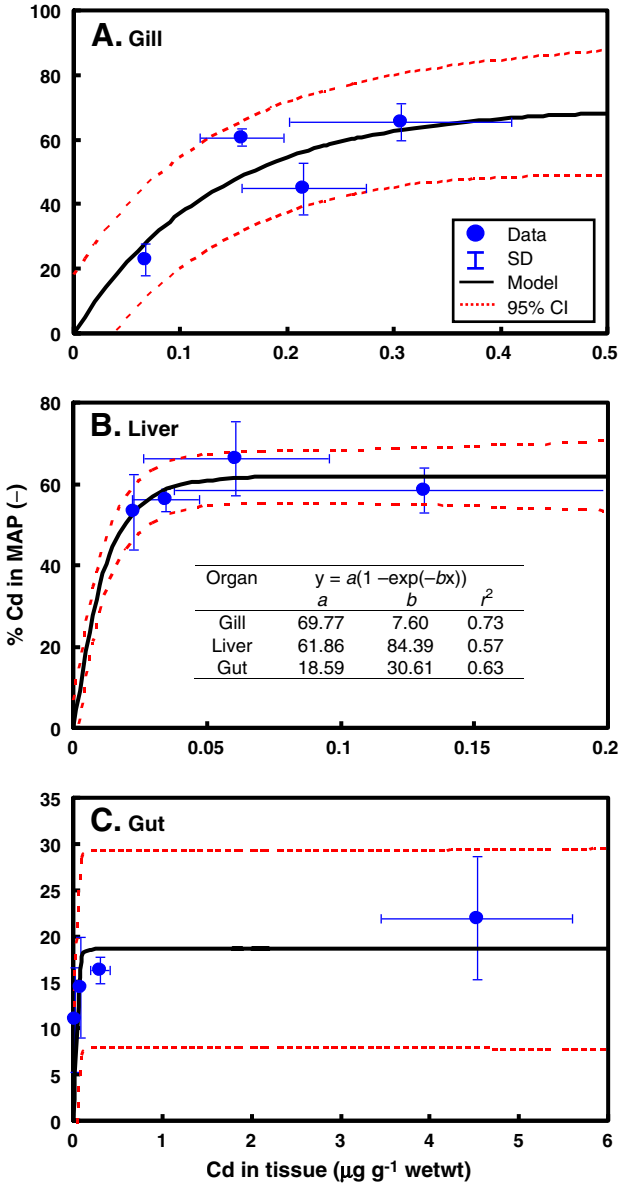

Fig. 4. Relationships between % Cd in metabolically active pool (MAP) and Cd in tissue of (A) gill, (B) liver, and (C) gut. Inset table shows the best-fitting model for dose–response relationships in target tissues. Error bars represent standard deviation from mean.

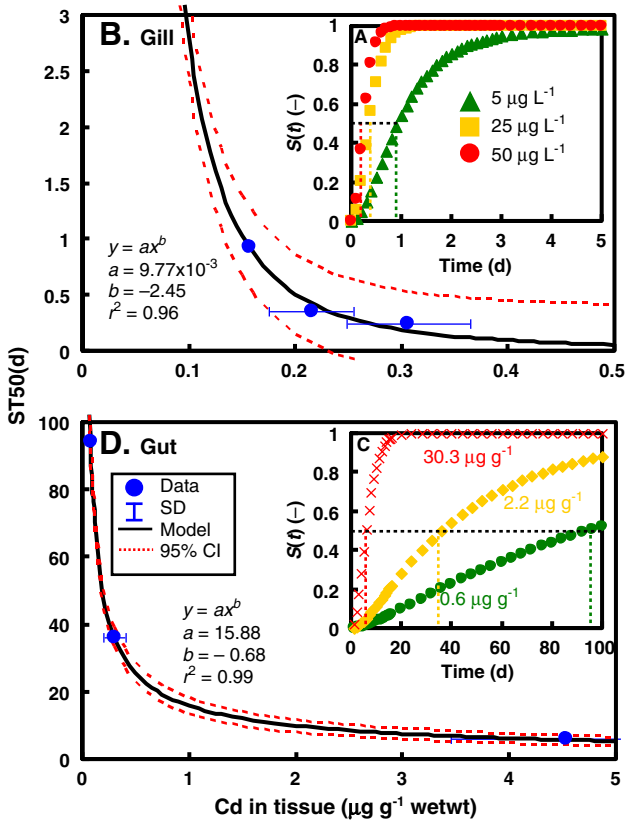

Fig. 5. Using DAM to calculate the time-dependent susceptibility risk probability $S(t)$ for (A) gill exposed to 5, 25, and 50 $\mu g\ L^{-1}$ Cd and (C) gut exposed to 0.6, 2.2, and 30.3 $\mu g\ g^{-1}$ Cd, and the dotted lines are marked for susceptibility time that causes 50% effect (ST50). And best-fitting model describing the relationships between ST50 and Cd in target tissues for (B) gill and (D) gut.

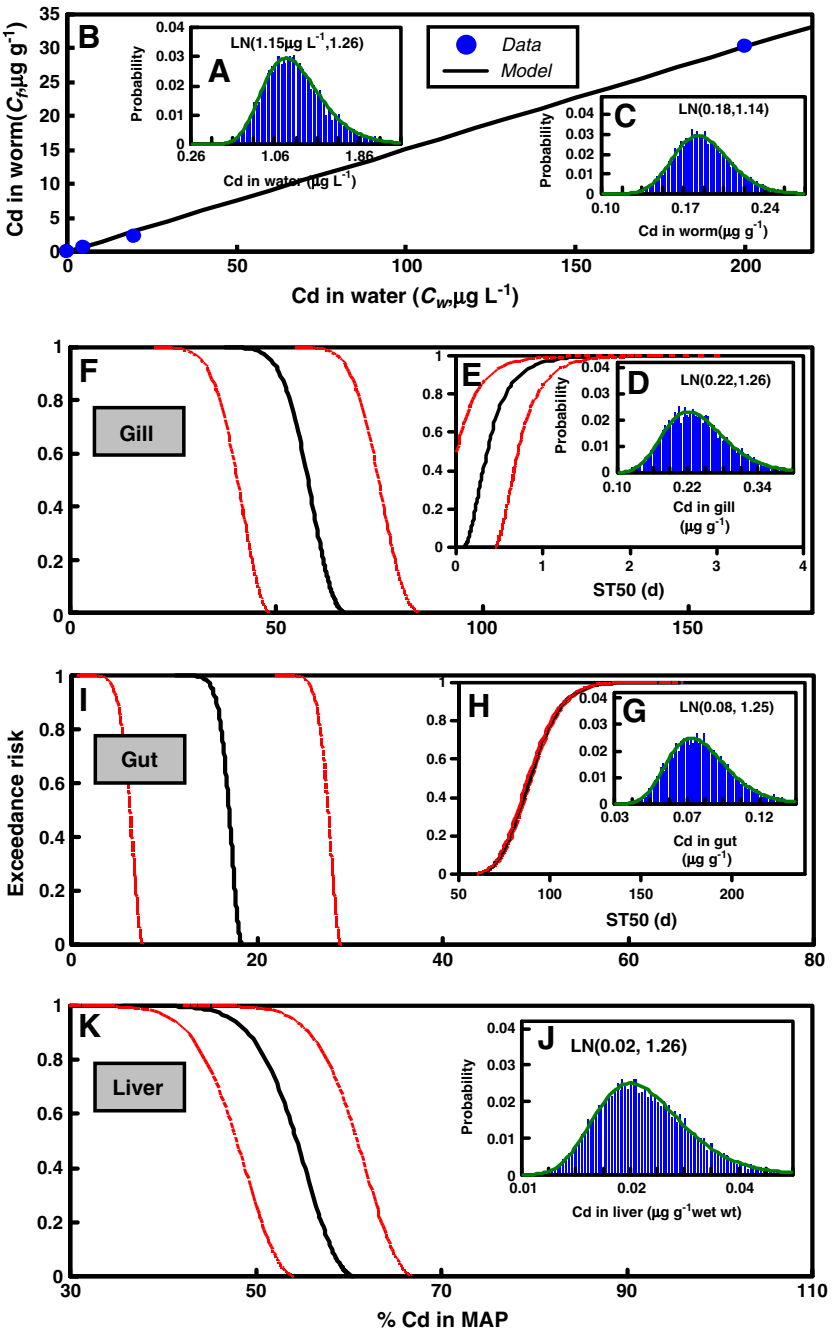

Fig. 6. (A) Environmentally relevant Cd concentration distribution in Taiwan (www.epa.gov.tw). (B) Linear relationship between Cd in water and in worm (data adopted from Ng and Wood, 2008). (C) Lognormal probability distribution of Cd in worm subject to environmental Cd distribution. A PBPK model was used to predict the steady-state Cd burden distribution (D, G, J) and estimating organ-specific Cd susceptibility exceedance risk probability of % Cd in MAP of (F) gill, (I) gut, and (K) liver as well as ST50 exceedance risk probability for (E) gill and (H) gut. LN(*a*, *b*) denotes the lognormal (LN) distribution with geometric mean *a* and geometric standard deviation *b*.

environmental Cd stress can be calculated as LN(0.18 μg g^{-1} wet wt, 1.14) (Fig. 6C). Given the estimated waterborne and dietborne Cd distributions (Fig. 6A, C) as inputs together with the essentially physiological parameters (see Appendix B) used in PBPK model for Cd–rainbow trout system, the equilibrium Cd burden distributions in gill, gut, and liver can be calculated (Fig. 6D, G, J). The organ-specific Cd susceptibility risk probability can then be estimated followed by Eqs. (7a) and (7b) (Fig. 6E, F, H, I, K).

Our results revealed that gill had a 95% probability of % Cd in MAP exceeding 49%; it is likely (70% probability) to have exceeded 55% Cd in MAP but is unlikely (30% probability) to have exceeded 60% (Fig. 6F; Table 3). The Cd susceptibility risk estimates of liver experienced the similar results of gill, indicating 47%, 52%, and 56% probabilities of % Cd in MAP corresponding to risks of 0.95, 0.7, and 0.3, respectively (Fig. 6K; Table 3). In contrast to gill and liver, gut had a relative lower Cd susceptibility risk probabilities (ranging from 15 to 17% Cd in MAP) (Fig. 6I; Table 3). The result also indicated that gut had a 95% probability of having exceeded 114 days of ST50 and a 70% probability of having exceeded 96 days. It is unlikely (30% probability) that ST50 of gut exceeded 82 days (Fig. 6H; Table 3). Gill, however, had relative lower ST50 risk estimates ranging from 0.27 to 0.90 day covering from 30% to 95% probabilities (Fig. 6E; Table 3).

Please cite this article as: Liao C-M, et al, Assessing the impact of waterborne and dietborne cadmium toxicity on susceptibility risk for rainbow trout, Sci Total Environ (2010), doi:10.1016/j.scitotenv.2010.10.044

Table 3
Cadmium susceptibility risk estimates for gill, gut, and liver of rainbow trout at 95% (most likely), 70% (likely), and 30% (unlikely) probabilities subject to environmentally relevant Cd concentration in Taiwan.

Endpoints	Susceptibility risk estimates		
	Risk = 0.95	Risk = 0.7	Risk = 0.3
Gill			
%MAP (%)	48.7 (31.7–65.8)[a]	55.0 (38.0–72.0)	60.1 (42.9–77.3)
ST50 (d)	0.90 (0.55–1.26)	0.48 (0.12–0.84)	0.27 (0–0.62)
Gut			
%MAP (%)	15.2 (4.5–25.8)	16.5 (5.8–27.2)	17.4 (6.7–28.1)
ST50 (d)	114.6 (113.7–115.6)	96.4 (95.4–97.3)	82.0 (81.1–82.9)
Liver			
%MAP (%)	47.4 (40.8–54.0)	52.4 (45.9–59.0)	56.2 (49.7–62.7)

[a] Value in parentheses denotes 95% CI.

4. Discussion

4.1. Mechanistic links among k_2, k_r, and k_d

In this study, 3 key parameters were determined to link bioaccumulation and coping mechanisms to assess Cd susceptibility risk for rainbow trout: the ability to eliminate Cd (k_2), the ability to detoxify Cd (k_d), and the ability to repair Cd-induced damage (k_r). We found a negative correlation between k_2 and k_d in liver and gut, indicating that increasing k_d can compensate for lower k_2. This finding suggests a potential tradeoff between the ability to eliminate Cd and the ability to detoxify it for liver and gut. A negative correlation between k_r and k_2 in gill and gut was also found, suggesting that compensation exists between the ability to eliminate Cd and the ability to recover the Cd-induced damage. Direct measurement of k_r is difficult: not much is known about the central mechanisms of damage recovery in a cell-scale. However, k_2 can be determined experimentally. Once k_2 is estimated, k_r can be predicted by the proposed DAM algorithm. This study also implicates that k_r and k_d can be predicted by the proposed $k_2 - k_d - k_r$ functional relationships in terms of known k_2.

Elimination rate constants appear to be a tissue-specific trend in this study. Gill had the relative higher capacity of elimination, whereas liver had the lowest elimination rate constant. Kraemer et al. (2005) reported that the elimination rate constants were estimated to be 0.024 d^{-1}, 0.012 d^{-1}, and 0.002 d^{-1}, in the gill, gut, and liver of juvenile yellow perch (*Perca flavescens*), respectively, in the field situations. In addition, we found uptake decreased and elimination increased with increasing exposure concentration in gill, whereas uptake and elimination decreased with increasing exposure concentration in liver (Table 1). McGeer et al. (2000) performed an experiment and applied an exponential equation to estimate the maximum accumulation and the biological half-life of Cd for rainbow trout exposed to 3 Cd μg L^{-1}. Based on their estimates, we could estimate the uptake and elimination rates of 321.8 mL g^{-1} d^{-1} and 0.25 d^{-1} for gill, 19.85 mL g^{-1} d^{-1} and 3.25×10^{-3} d^{-1} for liver, and 78.36 mL g^{-1} d^{-1} and 0.30 d^{-1} for whole body, respectively. Indeed, the higher uptake and lower elimination in gill and the higher uptake and elimination in liver were observed.

Zhang and Wang (2007) investigated the bioaccumulation of Cd in different juvenile sizes of marine black sea bream *Acantopagrus schlegeli* by fitting a toxicokinetic model. They indicated that the uptake rate constant decreased with increasing fish size, with uptake rate constants ranging from 1.43 to 14 mL g^{-1} d^{-1}. Moreover, the elimination rate constant of 0.089 d^{-1} could be estimated by applying compartmental analysis ($C_w = 0.05 - 0.2$ μg l^{-1}). Their estimates of parameter were also consistent with our study.

4.2. Subcellular partitioning implications

Kamunde (2009) reported that the rank of Cd accumulation in subcellular fractions in the gill of rainbow trout was: HSP > HLP > nuclei > microsomes–lysosomes ≥ mitochondria > resistant fraction, whereas for liver it was HSP > HLP > microsomes–lysosomes > mitochondria > nuclei > resistant fraction. Generally, Cd-induced toxicity could be linked to the increase of Cd in structure with essential metabolic roles in MAP such as mitochondria, nuclei, microsomes–lysosomes, and HLPs. If relative contribution of a metal-sensitive fraction to total cellular Cd burden remains constant or increases, detoxification cannot bring into play. On the other hand, if relative proportion decreases, some protection of this fraction may be evident. Our results suggested that a partial protection of some metal-sensitive sites was achieved by the initiation of cellular detoxification mechanisms in liver. Liver is the main detoxifying organ in all the animals and is the dominant accumulating organ for metal in fish. The metal concentration in fish hepatic tissue seems to be highly dependent on metal concentration in medium and exposure time.

The mechanism of Cd distribution in subcellular partioning is still not fully understood based on the limited published data. Recent studies indicated that Cd bound to MDP in freshwater fish liver ranged between 30% and 76.5%, whereas Cd associated with MAP and cellular debris fractions ranged from 21.52% to 59.85% and 10.21% to 33.68%, respectively (Olsson and Hogstrand 1987; Kraemer et al., 2006a,b). The percent Cd distribution differed among the subcellular partitioning in the following order: MDP > MAP > cellular debris. Thus, the MDP may play an important role to response to Cd toxicity effect in the aquatic fish level.

In contrast, Cd binding in gill-MAP increased as Cd in exposure medium increased, suggesting that gill tissue may be more susceptible to waterborne Cd toxicity relative to liver due to high amount of bioavailable Cd. For liver, Cd concentrations in HSP fraction increased with Cd, reaching high proportions of intracellular Cd (nearly 40–50%) when rainbow trout were exposed to high Cd of 50 μg L^{-1}.

Our results also indicated that average liver detoxification rate constant had nearly 5 order of magnitude higher than elimination rate constant, suggesting that metal-binding HSP play an important role in metal detoxification and can account for the partial protection of metal-sensitive sites discussed above. Quantitatively, our results showed that averaged k_d and k_2 estimates were respectively 1.13 and 0.41 d^{-1} for gill, and 1.1 and ~10^{-6} d^{-1} for liver when rainbow trout exposed to waterborne Cd ranging from 5 to 50 μg L^{-1}.

Ng and Wood (2008) reported that when rainbow trout exposed to dietborne Cd, a higher Cd concentration was associated with MAP, whereas dietary Cd exposure also caused potential toxicity to cells of stomach with more Cd bounding to HLPs. Ng and Wood (2008) also found that detoxification appeared to take place in the Cd-exposed rainbow trout because more Cd were bound to metallothionein-like proteins by week 4 of exposure. Based on our estimation, the averaged rate constants of k_d and k_2 were 34.41 and 0.13 d^{-1} for gut subjected to dietborne Cd ranging from 0.6 to 30.3 μg g^{-1} wet wt of worm.

4.3. Risk assessment implications

The ultimate goal of our analysis was to determine the probability distribution of susceptibility risk to an environmental stressor of Cd, conditioned upon the measurements in published database of Cd-rainbow trout system. In this study, we presented a probabilistic assessment approach for estimating Cd susceptibility risk for rainbow trout exposed to environmentally relevant Cd concentration. We constructed the dose–response models based on two endpoints of % Cd in MAP and susceptibility time that causes 50% effect (ST50). To do this, we used a well-established Cd-rainbow trout PBPK model to predict organ-specific steady-state Cd burdens. We concluded that % Cd in MAP for gill and liver was very likely to have exceeded 47–49%

Please cite this article as: Liao C-M, et al, Assessing the impact of waterborne and dietborne cadmium toxicity on susceptibility risk for rainbow trout, Sci Total Environ (2010), doi:10.1016/j.scitotenv.2010.10.044

and was likely to have been above 52–55%, though it is unlikely to have exceeded 56–60%. In contrast to gill and liver, gut had a relative lower Cd susceptibility risk estimates ranging from 15 to 17% Cd in MAP. Thus gut had longer ST50 values of 114, 96, and 82 days corresponding to 95%, 70%, and 30% probabilities, respectively.

Dietary accumulation can cause additional bioaccumulation, resulting in an increase in metal concentration with increasing trophic level in food webs (Meyer et al., 2005; Karimi et al., 2007; Croteau and Luoma, 2009; Lapointe et al., 2009). To identify bioaccumulative metals, regulatory authorizes much rely on BCFs measured in laboratory exposure assay or in the field. We anticipate that the proposed $k_2-k_d-k_r$ scheme derived based on the TK, the SPM, and the DAM could link the BCFs criteria to serve as an integrated predictive model for identifying bioaccumulative metals in aquatic organisms. We anticipate that the present study can provide a useful tool to identify and to assess metals that can bioaccumulate in food chains and achieve harmful concentrations in high-trophic level organisms including human beings.

Here we used the mechanistic ecotoxicology models to determine the influence of k_2, k_d, and k_r on metal bioaccumulation in aquatic food chains. The proposed probabilistic risk assessment framework can incorporate $k_2-k_d-k_r$ scheme to help government-based biomonitoring and bioassessment programs to prevent potential aquatic ecosystems and human health consequences.

Moreover, the present approach can also be used to develop species susceptibility risk distributions to estimate risk thresholds of toxicity for metal susceptible species that lack data (Brix et al., 2010). Species susceptibility risk distribution may analogous to species sensitivity distribution (SSD). SSD is a statistical cumulative distribution estimated from toxicity data for a set of species responses and can be used to extrapolate aquatic toxicity data to criteria to protect aquatic life and diverse freshwater ecosystems (Mebane, 2010; Brix et al., 2010).

In conclusion, recently developed toxicological modeling approaches for predicting metal toxicity to aquatic organisms were readily amenable to an integrated-scale analysis (Fiksel et al., 2009). Here we showed that such models could be derived from an integrated-scale analysis generated from four different types of functional relationship: the BLM, the DAM, and the PBPK models, and the SPM, both of key toxicological determinants involved and of functional connections between them.

Appendix A1. Schematic representation of Cd PBPK model in rainbow trout (see Appendix A2 and B for detailed meanings of symbols)

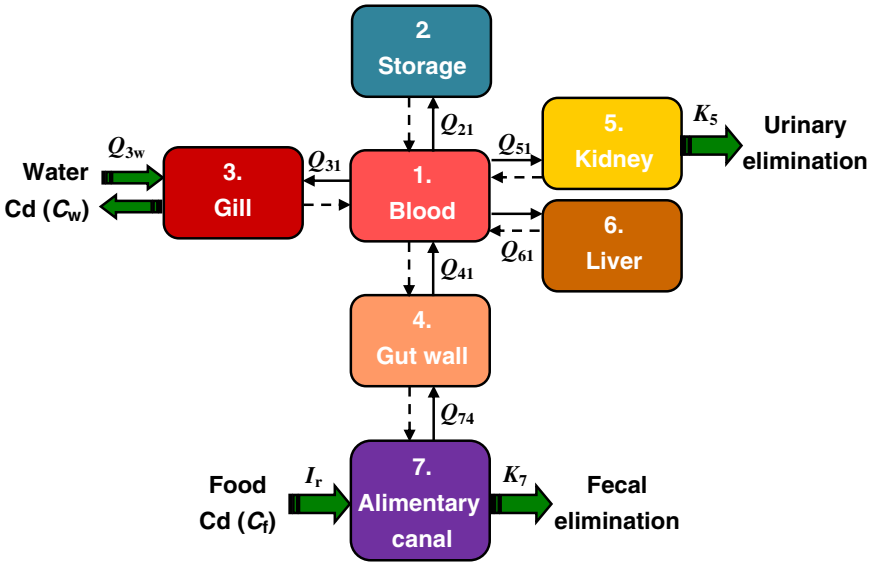

Appendix A2. The PBPK model equations

Compartment	Equation	
1. Blood (c_1, μg L^{-1})	$\frac{dB_1c_1}{dt} = Q_{21}\left(\frac{v_2}{p_2}-f_dc_1\right) + Q_{31}\left(\frac{v_3}{p_3}-f_dc_1\right) + Q_{41}\left(\frac{v_4}{p_4}-f_dc_1\right) + Q_{51}\left(\frac{v_5}{p_5}-f_dc_1\right) + Q_{61}\left(\frac{v_6}{p_6}-f_dc_1\right)$	(A2.1)
2. Storage (v_2, μg g^{-1})	$\frac{dw_2v_2}{dt} = Q_{21}\left(f_dc_1-\frac{v_2}{p_2}\right)$	(A2.2)
3. Gill (v_3, μg g^{-1})	$\frac{dw_3v_3}{dt} = Q_{3w}\left(\alpha_{w3}C_w-\frac{v_3}{p_3}\right) + Q_{31}\left(f_dc_1-\frac{v_3}{p_3}\right)$	(A2.3)
4. Gut wall (v_4, μg g^{-1})	$\frac{dw_4v_4}{dt} = Q_{41}\left(f_dc_1-\frac{v_4}{p_4}\right) + Q_{74}\left(\frac{v_7}{p_7}-b_{47}\frac{v_4}{p_4}\right)$	(A2.4)
5. Kidney (v_5, μg g^{-1})	$\frac{dw_5v_5}{dt} = Q_{51}\left(f_dc_1-\frac{v_5}{p_5}\right)-K_5w_5v_5$	(A2.5)
6. Liver (v_6, μg g^{-1})	$\frac{dw_6v_6}{dt} = Q_{61}\left(f_dc_1-\frac{v_6}{p_6}\right)$	(A2.6)
7. Alimentary canal (v_7, μg g^{-1})	$\frac{dw_7v_7}{dt} = I_rw_{total}C_f + Q_{74}\left(b_{47}\frac{v_4}{p_4}-\frac{v_7}{p_7}\right)-K_7w_{total}v_7$	(A2.7)

Please cite this article as: Liao C-M, et al, Assessing the impact of waterborne and dietborne cadmium toxicity on susceptibility risk for rainbow trout, Sci Total Environ (2010), doi:10.1016/j.scitotenv.2010.10.044

Appendix B Physiologically based parameters used in the PBPK model

Symbol	Value	Description (unit)
Physiologically based parameters[a]		
K_7	8.33×10^{-5}	Egestion rate from alimentary canal ($g\,g^{-1}\,h^{-1}$)
f_d	0.1	Fraction Cd dissolved in blood (–)
p_2	0.02	Storage partition coefficient ($L\,g^{-1}$)
p_3	0.65	Gill partition coefficient ($L\,g^{-1}$)
p_4	0.65	Gut wall partition coefficient ($L\,g^{-1}$)
p_5	620	Kidney partition coefficient ($L\,g^{-1}$)
p_6	0.2	Liver partition coefficient ($L\,g^{-1}$)
p_7	6.5	Alimentary canal partition coefficient ($L\,g^{-1}$)
α_{w3}	6	Gill sorption factor: enhanced surface sorption (–)
b_{47}	7	Bile factor: enhanced exchange gut to alimentary canal (–)
Weight-adjusted physiological parameter		
w_{total}	13.28	Weight of whole body (g)
B_1	6.64×10^{-4}	Blood volume (L)
w_2	11.48	Weight of storage (g)
w_3	0.48	Weight of gill (g)
w_4	0.73	Weight of gut wall (g)
w_5	0.10	Weight of kidney (g)
w_6	0.17	Weight of liver (g)
w_7	0.07	Weight of alimentary canal (g)
K_5	1.17×10^{-4}	Kidney excretion rate (d^{-1})
Q_{3w}	3.32×10^{-4}	Gill-water exchange ($L\,d^{-1}$)
Q_{21}	0.66	Storage-blood exchange ($L\,d^{-1}$)
Q_{31}	0.01	Gill-blood exchange ($L\,d^{-1}$)
Q_{41}	0.017	Gut-blood exchange ($L\,d^{-1}$)
Q_{51}	1.67×10^{-3}	Kidney-blood exchange ($L\,d^{-1}$)
Q_{61}	5.10×10^{-3}	Liver-blood exchange ($L\,d^{-1}$)
Q_{74}	0.245	Alimentary canal-gut exchange ($L\,d^{-1}$)

[a]Adopted from Thomann et al. (1997).

Appendix C Affinity constants and related parameter used in BLM

BLM used parameter	
Affinity constants (M^{-1})	
$\log K_{CdBL}$	8.6[a]
$\log K_{CaBL}$	4.5[b]
$\log K_{HBL}$	6.7[a]
$\log K_{NaBL}$	3[b]
$\log K_{MgBL}$	3.2[b]
BLM parameter	
[a]	34.65

[a]Adopted from Playle et al. (1993).
[b]Adopted from Santore et al. (2002).

References

Alquezar R, Markich SJ, Twining JR. Uptake and loss of dissolved ^{109}Cd and ^{75}Se in estuarine macroinvertebrates. Chemosphere 2007;67:1202–10.

Alquezar R, Markich SJ, Twining JR. Comparative accumulation of ^{109}Cd and ^{75}Se from water and food by an estuarine fish (*Tetractenos glaber*). J Environ Radioactiv 2008;99:167–80.

Ashauer R, Boxall ABA, Brown CD. New ecotoxicological model to simulate survival of aquatic invertebrates after exposure to fluctuating and sequential pulses of pesticides. Environ Sci Technol 2007;41:1480–6.

Bielmyer GK, Grosell M, Paquin PR, Mathews R, Wu KB. Validation study of the acute biotic ligand model for silver. Environ Toxicol Chem 2007;26:2241–6.

Brix KV, Keithly J, Santore RC, DeForest DK, Tobiason S. Ecological risk assessment of zinc from stormwater runoff to an aquatic ecosystem. Sci Total Environ 2010;408:1824–32.

Clearwater SJ, Farag AM, Meyer JS. Bioavailability and toxicity of dietborne copper and zinc to fish. Comp Biochem Physiol 2002;132C:269–313.

Croteau MN, Luoma SN. Predicting dietborne metal toxicity from metal influxes. Environ Sci Technol 2009;43:4915–21.

Curis E, Nicolis I, Bensaci J, Deschamps P, Bénazeth S. Mathematical modeling in metal metabolism: overview and perspectives. Biochimie 2009;91:1238–54.

De Schamphelaere KAC, Janssen CR. A biotic ligand model predicting acute copper toxicity for Daphnia magna: the effects of calcium, magnesium, sodium, potassium, and pH. Environ Sci Technol 2002;36:48–54.

Dubois M, Hare L. Subcellular distribution of cadmium in two aquatic invertebrates: change over time and relationship to Cd assimilation and loss by a predatory insect. Environ Sci Technol 2009;43:356–61.

Fairbrother A, Wenstel R, Sappington K, Wood W. Framework for metals risk assessment. Ecotoxicol Environ Saf 2007;68:145–227.

Fiksel J, Graedel T, Hecht AD, Rejeski D, Sayler GS, Senge PM, et al. EPA at 40: bringing environmental protection into the 21st century. Environ Sci Technol 2009;43:8716–20.

Gimbert F, Vijver MG, Coeurdassier M, Scheifler R, Peijnenburg WJGM, Badot PM, de Vaufleury A. How subcellular partitioning can help to understand heavy metal accumulation and elimination kinetics in snails. Environ Toxicol Chem 2008;27:1284–92.

Gundogdu A, Harmantepe FB, Dogan G, Karsli Z, Asci MY. Effects of dietborne copper on accumulation in the tissues and organs, growth and feed utilization of rainbow trout (*Oncorhynchus mykiss*, Walbaum, 1792) juvenile. J Anim Vet Adv 2009;8:2495–502.

Hartung T. Toxicology for the twenty-first century. Nature 2009;460:208–12.

Kamunde C. Early subcellular partitioning of cadmium in gill and liver of rainbow trout (*Oncorhynchus mykiss*) following low-to-near-lethal waterborne cadmium exposure. Aquat Toxicol 2009;91:291–301.

Karimi R, Chen CY, Pickhardt PC, Fisher NS, Folt CL. Stoichiometric controls of mercury dilution by growth. Proc Natl Acad Sci USA 2007;104:7477–82.

Kraemer LD, Campbell PGC, Hare L. A field study examining metal elimination kinetics in juvenile yellow perch (*Perca flavescens*). Aquat Toxicol 2005;75:108–26.

Kraemer LD, Campbell PGC, Hare L. Seasonal variations in hepatic Cd and Cu concentrations and in the sub-cellular distribution of these metals in juvenile yellow perch (*Perch flavescens*). Environ Pollut 2006a;142:313–25.

Kraemer LD, Campbell PGC, Hare L, Auclair JC. A field study examining the relative importance of food and water as sources of cadmium for juvenile yellow perch (*Perch flavescens*). Can J Fish Aquat Sci 2006b;63:549–57.

Kraemer LD, Campbell PGC, Hare L. Modeling cadmium accumulation in indigenous yellow perch (*Perca flavescens*). Can J Fish Aquat Sci 2008;65:1623–34.

Lapointe D, Gentes S, Ponton DE, Hare L, Couture P. Influence of prey type on nickel and thallium assimilation, subcellular distribution and effects in juvenil fathead minnows (*Pimephales promelas*). Environ Sci Technol 2009;43:8665–70.

Lee JH, Landrum PF, Koh CH. Prediction of time-dependent PAH toxicity in *Hyalella azteca* using a damage assessment model. Environ Sci Technol 2002;36:3131–8.

McGeer JC, Szebedinszky C, McDonald DC, Wood CM. Effects of chronic sublethal exposure to waterborne Cu, Cd or Zn in rainbow trout 2: tissue specific metal accumulation. Aquat Toxicol 2000;50:245–56.

Mebane CA. Relevance of risk predictions derived from a chronic species sensitivity distribution with cadmium to aquatic populations and ecosystems. Risk Anal 2010;30:203–23.

Menzie CA, Ziccardi LM, Lowney YW, Fairbrother A, Shock SS, Tsuji JS, et al. Importance of considering the framework principles in risk assessment for metals. Environ Sci Technol 2009;43:8478–82.

Meyer JS, Adams WJ, Brix KV, Luoma SN, Mount DR, Stubblefield WA, et al, editors. Toxicity of dietborne metals to aquatic organisms. Pensacola (FL), USA: Society of Environmental Toxicology and Chemistry (SETAC); 2005.

Ng TYT, Wood CM. Trophic transfer and dietary toxicity of Cd from the oligochaete to the rainbow trout. Aquat Toxicol 2008;87:47–59.

Olsson PE, Hogstrand C. Subcellular-distribution and binding of cadmium to metallothionein in tissues of rainbow-trout after exposure to Cd-109 in water. Environ Toxicol Chem 1987;6:867–74.

Playle RC, Dixon DG, Burnison K. Copper and cadmium binding to fish gill: estimates of metal-gill stability constants and modelling of metal accumulation. Can J Fish Aquat Sci 1993;50:2678–87.

Ponton DE, Hare L. Nickel dynamics in the lakewater metal biomonitor *Chaoborus*. Aquat Toxicol 2010;96:37–43.

Renner R. A tale of two fish. Environ Sci Technol 2008;42:6784–5.

Santore RC, Mathew R, Paquin PR, Di Toro D. Application of the biotic ligand model to predicting zinc toxicity to rainbow trout, fathead minnow, and *Daphnia magna*. Comp Biochem Physiol 2002;133C:271–85.

Schwartz ML, Vigneault B. Development and validation of a chronic copper biotic ligand model for *Ceriodaphnia dubia*. Aquat Toxicol 2007;84:247–54.

Tan XY, Luo Z, Zhang GY, Liu XJ, Jiang M. Effect of dietary cadmium level on the growth, body composition and several hepatic enzymatic activities of juvenile yellow catfish, *Pelteobagrus fulvidraco*. Aquac Res 2010;41:1022–9.

Thomann RV, Shkreli F, Harrison S. A pharmacokinetic model of cadmium in rainbow trout. Environ Toxicol Chem 1997;16:2268–74.

Tsai JW, Chen WY, Ju YR, Liao CM. Bioavailability links mode of action can improve the long-term field risk assessment for tilapia exposed to arsenic. Environ Int 2009;35:727–36.

Wang WX, Rainbow PS. Subcellular partitioning and the prediction of cadmium toxicity to aquatic organisms. Environ Chem 2006;3:395–9.

Wang M, Wang WX. Cadmium toxicity in a marine diatom as predicted by the cellular metal sensitive fraction. Environ Sci Technol 2008;42:940–6.

Zhang L, Wang WX. Size-dependence of the potential for metal biomagnifications in early life stages of marine fish. Environ Toxicol Chem 2007;26:787–94.

Please cite this article as: Liao C-M, et al, Assessing the impact of waterborne and dietborne cadmium toxicity on susceptibility risk for rainbow trout, Sci Total Environ (2010), doi:10.1016/j.scitotenv.2010.10.044